^{13}C NMR Spectroscopy Studies of Branching and Sequence Distribution in Copolymers of Vinyl Acetate and *n*-Butyl Acrylate Prepared by Semibatch Emulsion Copolymerization

David Britton,[†,§] Frank Heatley,[‡] and Peter A. Lovell[*,†]

Polymer Science and Technology Group, Manchester Materials Science Centre, University of Manchester and UMIST, Grosvenor Street, Manchester, M1 7HS, United Kingdom, and Department of Chemistry, University of Manchester, Manchester, M13 9PL, United Kingdom

Received May 23, 2000; Revised Manuscript Received November 10, 2000

ABSTRACT: ^{13}C NMR spectroscopy has been used to study branching and sequence distributions in copolymers of vinyl acetate (VAc) and *n*-butyl acrylate (BA) prepared by semibatch emulsion copolymerization. All copolymerizations proceeded via a seed stage that was carried out under monomer-flooded conditions, followed by a growth stage that operated under monomer-starved conditions. The ^{13}C NMR spectra of the copolymers have been fully interpreted both in terms of the structural features arising from chain transfer to polymer and the repeat unit sequence distributions. The sequence distributions for copolymers formed in the seed stage are in reasonable agreement with predictions from the standard terminal-unit first-order Markov statistical model, showing that normal copolymerization kinetics operate under monomer-flooded conditions. However, the sequence distributions for copolymers produced in the growth stage are closely represented by a random Bernoullian distribution, showing that copolymers with random repeat unit sequence distributions are formed under monomer-starved conditions. The only reasonable explanation of this observation is that propagation is subject to diffusion control under monomer-starved conditions. The branching data reveal a synergistic effect in which the inclusion of only small amounts of either monomer leads to disproportionate increases in the level of branching. This is a consequence of the efficacy of H-abstraction at BA backbone tertiary C−H bonds by the highly reactive VAc-ended chain radicals. The results indicate that radicals with VAc end units abstract hydrogen atoms from BA repeat units about 7−8 times more rapidly than from VAc repeat units and that radicals with VAc end units are about 3−4 times as effective in abstracting hydrogen atoms from BA repeat units than are radicals with BA end units. Copolymer composition drift occurs in the seed stage due to the monomer-flooded conditions and results in virtually all of the BA being consumed before the conversion is high enough for chain transfer to polymer to become significant; hence, branching arises almost exclusively from H-abstractions by radicals with VAc end units. However, in the monomer-starved growth stage, radicals with BA end units and radicals with VAc end units both contribute to chain transfer to polymer in proportions that correspond to the composition of the comonomer feed; this observation again is consistent with diffusion control of propagation under monomer-starved conditions.

Introduction

In previous papers, we reported studies of chain transfer to polymer in bulk, solution, and emulsion free-radical polymerizations of vinyl acetate (VAc)[1,2] and *n*-butyl acrylate (BA)[3−6] in which NMR spectroscopy was used to detect structural features arising from chain transfer to polymer. The unique resonances thus identified were used to establish the chemistry of chain transfer to polymer and to quantify the level of branching in the polymers produced. In this way, we established that chain transfer to polymer in free-radical polymerizations of VAc proceeds principally via H-abstraction from the methyl side group with only a minor contribution from H-abstraction at backbone tertiary C−H bonds (see Scheme 1) and that chain transfer to polymer occurs more extensively in free-radical polymerizations of BA, proceeding via abstraction of hydrogen atoms from backbone tertiary C−H bonds (see Scheme 2). The rationales for these observations are discussed in the previous papers and, therefore, will not be repeated here.

The aim of the work described in the present paper was to use NMR spectroscopy to study chain transfer to polymer in emulsion copolymerizations of VAc and BA, the motivation being that such copolymerizations are of commercial importance.[7] ^{13}C NMR spectra of VAc/BA copolymers have been reported previously,[8−10] and assignments of resonances to compositional dyads and triads have been made. The VAc-centered triad probabilities were shown to be accessible with reasonable clarity from the spectrum of the backbone CH carbon in VAc units, which occurs as an individual group of peaks at 65−74 ppm. However, the dyad probabilities and the BA-centered triad probabilities were accessible only with difficulty from a complex, strongly overlapping pattern in the 33−43 ppm region comprising backbone CH_2 carbons from both VAc and BA units and backbone CH carbons from BA units. In this work, we have taken advantage of the higher sensitivity and resolution available from use of a considerably higher resonance frequency, to extend the ^{13}C NMR analysis of VAc/BA copolymers in two ways. First, the nature and extent of chain transfer to polymer have been characterized, and second, we have used the DEPT technique[11] to obtain CH and CH_2 subspectra of the 33−43 ppm region from which dyad and triad probabilities could be obtained much more clearly than hitherto. In both cases

* To whom correspondence should be addressed.
† Polymer Science and Technology Group.
‡ Department of Chemistry.
§ Current address: Rhodia Industrial Specialties, Ashton New Road, Clayton, Manchester, M11 4AT, United Kingdom.

10.1021/ma000901s CCC: $20.00
Published on Web 01/19/2001

Scheme 1. Mechanisms of Chain Transfer to Polymer in Free-Radical Homopolymerization of Vinyl Acetate (Carbons Labeled A, α, and β Are Described in the Discussion)

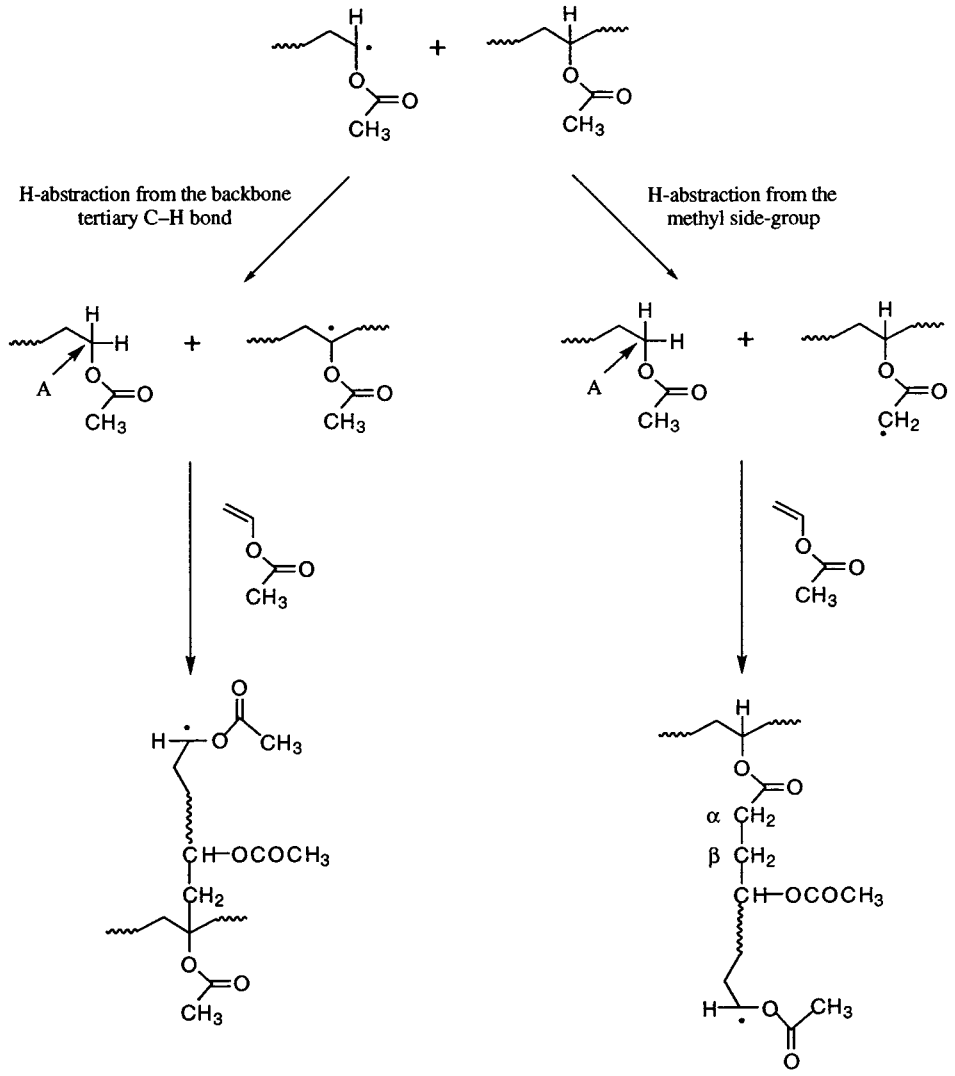

the results have been correlated with comonomer composition and the conditions of emulsion copolymerization.

Experimental Section

Purification of Reagents. VAc (Aldrich, >99%) and BA (Aldrich, >99%) were washed three times with dilute sodium hydroxide solution to remove the phenolic inhibitor, followed by washing thoroughly with water before drying over anhydrous calcium chloride. Water was deionized by passage through a series of Milli-RO6 (Millipore) ion-exchange columns. Ammonium persulfate (BDH, 99.5%), sodium bicarbonate (BDH, 99.0%), Aerosol OT-75 (Cytec), and hydroquinone (Aldrich, 99%) were used as supplied.

Emulsion Polymerizations. Table 1 gives the formulation used for the emulsion copolymerizations which were performed under a flowing nitrogen atmosphere at 70 °C on scales of approximately 2 dm^3 in flanged reaction vessels. The seed-stage water (less 45 g), Aerosol OT-75, and sodium bicarbonate were weighed into the reaction vessel which then was equipped with a nitrogen inlet, condenser, and mechanical stirrer before being placed in a water bath thermostated at 70 ± 1 °C. A steady flow of nitrogen was established while the surfactant/buffer solution attained the bath temperature, after which the seed-stage monomer mixture was added. When the temperature had stabilized, a solution of the seed-stage ammonium persulfate in water (40 g) was added and washed into the reaction vessel with a further quantity of water (5 g). The seed-stage reaction was allowed to proceed for 60 min before beginning the growth stage, in which a solution of the growth-stage Aerosol OT-75 in the growth-stage monomer mixture was metered into the reaction vessel at a controlled rate of 2.9 g min^{-1} over a period of 240 min using a Watson-Marlow 505S peristaltic pump. At 60, 120, and 180 min from the beginning of the seed stage, further quantities of ammonium persulfate (1.00 g) in water (40 g) were added and washed in with water (5 g). On completion of the growth-stage addition, a further 60 min reaction time was allowed before cooling the latex to room temperature and passing it through a 53 μm sieve.

A series of copolymerizations were carried out using mixtures of VAc and BA comprising 0, 5, 10, 15, 20, 40, 60, 80, and 100 wt % BA. For each copolymerization, aliquots (ca. 10 cm^3) were removed at the end of the seed stage and at 30 min intervals thereafter. To quench the reaction, each aliquot was transferred directly to a sample bottle which was placed in an ice/water bath and contained a preweighed quantity (ca. 0.3 g) of a 1% aqueous hydroquinone solution. The aliquots were used to monitor the conversion and the degree of branching. Conversions were determined from duplicate measurements of solids content using a mass-balance approach to account for previously removed aliquots and nonpolymeric solids. Samples for analysis by NMR spectroscopy were prepared as follows: (i) dialysis of the latex (contained in Visking tubing) against an approximately 1000 times excess of deionized water for a minimum of 10 days with at least one change of water each day, (ii) freeze−thaw cycling of the

Scheme 2. Mechanism of Chain Transfer to Polymer in Free-Radical Homopolymerization of *n*-Butyl Acrylate (Carbons Labeled B and C Are Described in the Discussion)

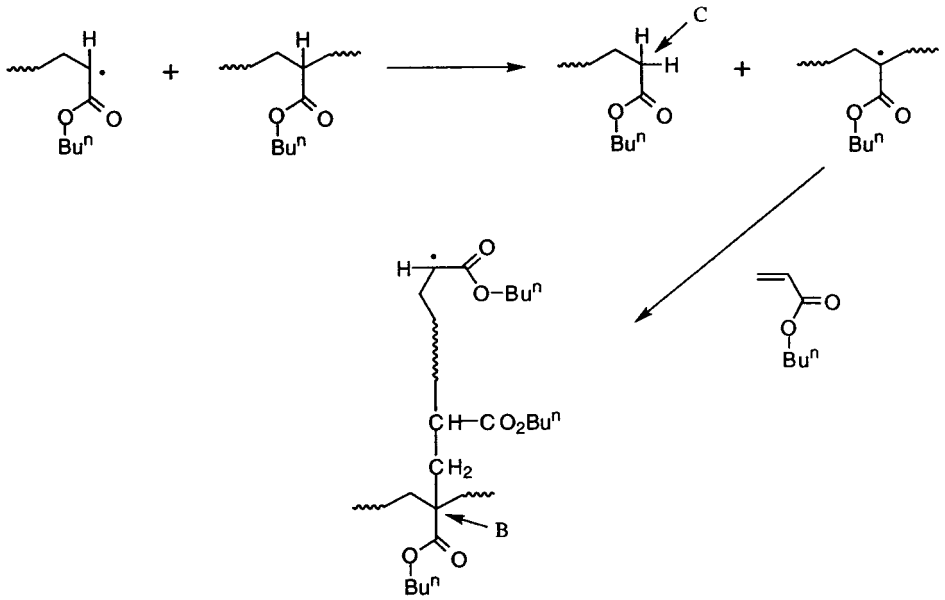

dialyzed latex until complete coagulation resulted, (iii) decanting of the supernatant from the coagulated polymer before washing with deionized water and drying to constant weight at 60 °C under vacuum, and (iv) transfer of the dried polymer to the NMR tube.

NMR Spectroscopy. ^{13}C NMR spectra were recorded at 23 ± 1 °C using a Varian Associates Unity 500 spectrometer operating at 125.8 MHz. Samples of the copolymers were dissolved in $CDCl_3$ to give solutions of concentration ca. 100 mg cm^{-3}. Chemical shifts were referenced to the solvent peak at 77 ppm. To maximize the signal-to-noise ratio in a given time, spectra were normally run with continuous ^1H decoupling using a pulse interval of 0.5 s and a pulse flip angle of 70°. Under these rapid pulse conditions, the relative intensities may not necessarily reflect the relative abundance of each type of carbon because of differential relaxation times and nuclear Overhauser enhancements (NOE). In particular, the intensities of primary and quaternary carbons are underestimated relative to CH and CH_2 carbons. To check the quantitative accuracy of these fast pulse spectra, some samples were analyzed again with NOE suppression by inverse gated decoupling[12] and with a pulse interval of 10.5 s to allow complete recovery of all carbons. Additionally, the DEPT technique[11] was used to determine the multiplicity of the peaks, i.e., whether a carbon was primary, secondary, tertiary, or quaternary, and to obtain CH and CH_2 subspectra from which monomer sequence distributions were obtained.

The mol % branches data were calculated either from quantitative spectra recorded using both NOE suppression with full relaxation or from fast pulse spectra, in each case using the following equations,

$$\text{mol \% VAc ends } (\%V_{\text{ends}}) = \frac{100 \times \text{Corr}_{\text{VAc}} \times I_{60-62}}{I_{60-75}} \quad (1)$$

$$\text{mol \% BA branches } (\%B_{\text{Cq}}) = \frac{100 \times \text{Corr}_{\text{BA}} \times I_{45-48}}{I_{60-75}} \quad (2)$$

where Corr_{VAc} and Corr_{BA} are correction factors that account for differences in longitudinal relaxation times and NOE for fast pulse spectra, and I_{X-Y} denotes the integrals for the $X \le \delta_C \le Y$ regions of the spectra: I_{45-48} includes all C_q carbons in branched BA repeat units; I_{60-62} includes all $-CH_2(OAc)$ end group carbons; and I_{60-75} is the sum of the $-CH_2(OAc)$ end group carbons, $-OCH_2-$ BA side-group carbons, and backbone CH−O carbons in VAc repeat units. Mean values of the correction factors were determined from analysis of spectra for each of the final copolymers from the 5, 10, and 20 wt % BA emulsion copolymerizations recorded (i) under fast pulse conditions and (ii) using both NOE suppression with full relaxation; the mean values obtained were $\text{Corr}_{\text{VAc}} = 0.9$ (±0.1) and $\text{Corr}_{\text{BA}} = 2.5$ (±0.2). Obviously, for analysis of the spectra recorded under quantitative conditions, $\text{Corr}_{\text{VAc}} = \text{Corr}_{\text{BA}} = 1$. The $\%V_{\text{ends}}$ and $\%B_{\text{Cq}}$ data were normalized to their respective repeat unit contents in the copolymer using the following equations,

Table 1. Formulation for Emulsion Copolymerization of VAc and BA (~2 dm^3 Scale)

formulation component	seed stage (mass/g)	growth stage (mass/g)
monomer mixture	135.0	675.0
deionized water	1215.0	135.0
Aerosol OT-75	9.30	24.83
sodium bicarbonate	0.90	
ammonium persulfate	1.00	3.00

$$\text{\% of VAc repeat units that are at chain ends } (\%V_{\text{ends}}/V) = \frac{\%V_{\text{ends}}}{F_{\text{VAc}}} \quad (3)$$

$$\text{\% of BA repeat units that are branched } (\%B_{\text{Cq}}/B) = \frac{\%B_{\text{Cq}}}{F_{\text{BA}}} \quad (4)$$

where F_{VAc} and F_{BA} are the cumulative mole fractions of VAc and BA repeat units present in the copolymer sample analyzed. Since all samples were taken at points in the reaction when the instantaneous conversion was very high, F_{VAc} and F_{BA} were taken as equal to the respective mole fractions of VAc and BA in the comonomer mixture.

Results and Discussion

Assignment of NMR Spectra. As expected, the copolymer spectra showed features common to those reported in detail previously for spectra of poly(vinyl acetate) (PVAc)[1] and poly(*n*-butyl acrylate) (PBA)[6] homopolymers. A representative copolymer spectrum is shown in Figure 1. For the purposes of the present studies, the 58−74 and 30−50 ppm regions of the spectra are the most important and show the following

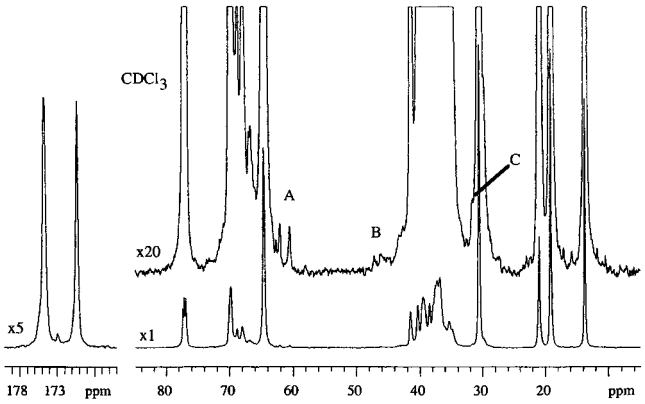

Figure 1. ^{13}C NMR spectrum of the final sample from a VAc/BA (60 wt % BA) copolymerization.

significant features in relation to the chemistry of chain transfer to polymer (cf. Schemes 1 and 2).

(i) The small peak at 60.5 ppm (peak A) has also been observed in spectra of PVAc[1] and is assigned, for the same reasons as given in that paper, to the ultimate CH_2 carbon in a $-CH_2CH(OAc)CH_2CH_2(OAc)$ end group (see Scheme 1). This peak is clear evidence for termination of VAc radical ends by H-abstraction.

(ii) Similarly, the small peak at 31.5 ppm (peak C) has previously been observed in spectra of PBA[6] and so is assigned, using the same reasoning as given in that paper, to the ultimate CH_2 carbon in a $-CH_2CH(COOBu)CH_2CH_2(COOBu)$ end group (see Scheme 2). This peak provides clear evidence for termination of BA radical ends by H-abstraction.

(iii) There is no indication of quaternary carbon peaks in the region 80 ppm or higher, indicating that chain transfer to polymer via abstraction of a CHOAc backbone tertiary hydrogen is negligible, an observation that is consistent with previous studies of PVAc. [1]

(iv) The α and β CH_2 carbons arising from chain transfer to the acetyl methyl group in VAc units (see Scheme 1) are predicted to occur at 30 and 34 ppm[1] but are obscured by side-group and backbone CH_2 carbons in BA units and, for copolymers with higher VAc contents, by peaks from inverted sequences of VAc repeat units.[1]

(v) Quaternary carbon peaks (peaks B) were detected in the region 44−48 ppm at chemical shifts which varied from 44 ppm (at 5 wt % BA) to 48 ppm (at 80 wt % BA). These peaks were assigned to the quaternary carbon generated by chain transfer to polymer involving abstraction of the BA $CHCOOC_4H_9$ tertiary hydrogen (see Scheme 2), as observed in previous studies of BA homopolymers and copolymers.[3−6] The variation in chemical shift is attributed to the fact that the neighbors of the quaternary carbon would vary from mainly VAc units in copolymers with low BA contents to mainly BA units in copolymers with high BA contents. In PBA homopolymer, this carbon was found at 48 ppm for spectra run, as in the present work, using $CDCl_3$ as the solvent. [6]

Figure 2 compares expansions of the 60−71 ppm region for three copolymers. The OCH_2 carbon in the side-chain of BA units at 64.3 ppm is clearly resolved from the backbone CH carbons in VAc units at 65−71 ppm. The indicated assignment of the VAc CH peaks to VAc-centered triads is described later in the section on monomer sequence distributions. For the analysis of chain transfer events, the significant peaks in this

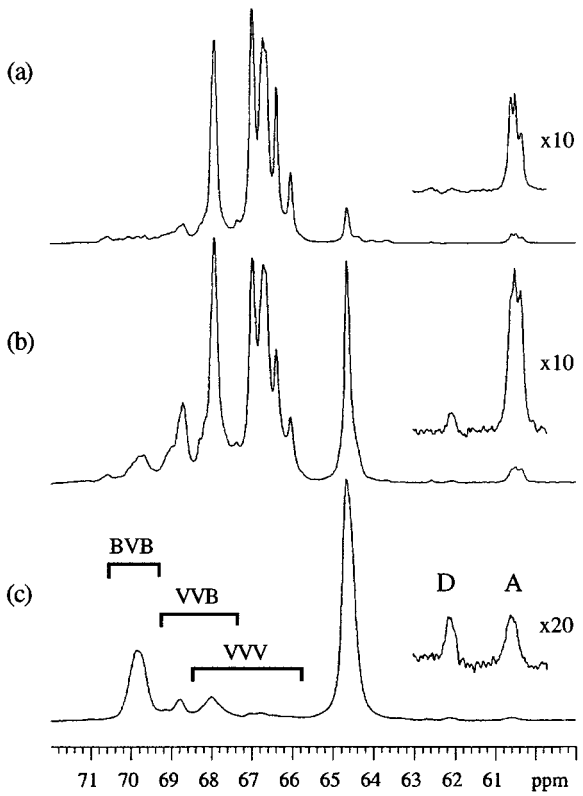

Figure 2. Expansions of the 60−71 ppm region of the ^{13}C NMR spectra of final samples from VAc/BA copolymerizations: (a) 5 wt % BA; (b) 20 wt % BA; (c) 60 wt % BA.

region are the small peaks A and D at ca. 60.5 and 62 ppm, respectively. As explained in point i above, peak A is assigned to the ultimate CH_2 carbon in a $-CH_2CH(OAc)CH_2CH_2(OAc)$ end group. Peak D is assigned to the ultimate CH_2 carbon in a $-CH_2CH(COOBu)CH_2CH_2(OAc)$ end group for the following reasons.

(a) DEPT spectra show that it is a CH_2 carbon.

(b) Its NMR relaxation properties (line width, NOE enhancement) are similar to those of peak A and consistent with a polymeric origin.

(c) Its chemical shift is higher by 1.5 ppm than that of peak C, a value consistent with that expected from substituent chemical shift increment tables[13] for replacing an $-OCOR$ group in a δ-position with a $-COOR$ group.

(d) Its intensity varied systematically with copolymer composition and reaction time in a manner that is consistent with such an assignment. This variation is illustrated by the representative spectra in Figure 2, which show the steady increase in the relative intensity of peak D as the BA content increases.

For reasons similar to those just described for CH_2 carbons in terminal $CH_2(OAc)$ groups, distinct peaks for CH_2 carbons in terminal $CH_2(COOBu)$ groups that have the structures $-CH_2CH(COOBu)CH_2CH_2(COOBu)$ and $-CH_2CH(OAc)CH_2CH_2(COOBu)$ can be expected, with the latter being some 2 ppm more shielded. As explained in point ii above, the resonance for the terminal $CH_2(COOBu)$ in the all-BA end structure is observed at 31.5 ppm (peak C); resolution of the terminal $CH_2(COOBu)$ in the VAc−BA end structure, however, is hindered by the presence of a nearby intense butyl side-group CH_2 peak at 30.6 ppm. Nevertheless, there is evidence in the spectra for its existence, as illustrated in Figure 3, which compares spectra in the 27−33 ppm

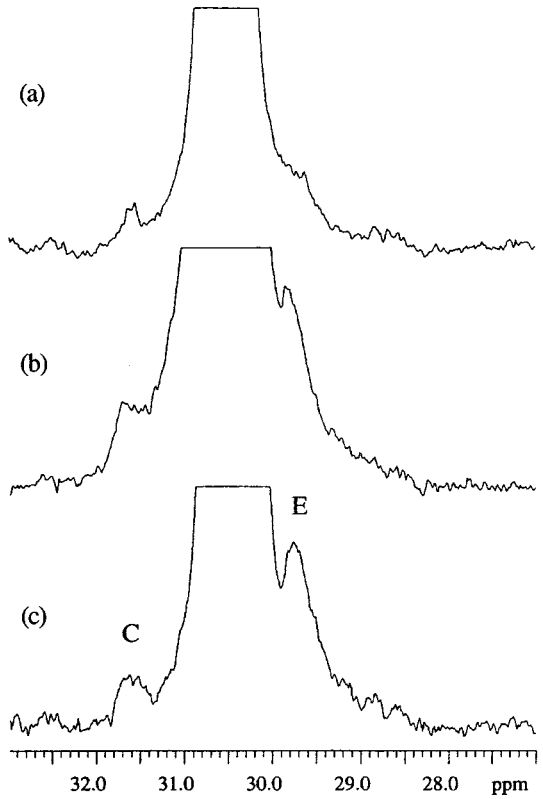

Figure 3. Expansions of the 27−33 ppm region of the ^{13}C NMR spectrum for samples taken from a copolymerization with 60 wt % BA: (a) 58 min (seed stage); (b) 178 min (midpoint in the growth stage); (c) 360 min (final copolymer).

region for 60 wt % BA copolymers obtained at different reaction times. There is a small peak (E) at the expected position, which also is observed in other copolymers and whose relative intensity increases systematically with reaction time and BA content. Unfortunately, the proximity of the intense butyl side-group CH_2 resonance to peaks C and E prevents accurate quantification of the terminal CH_2(COOBu) groups.

Emulsion Copolymerization Conversion−Time Curves. The formulation and procedure used for the emulsion copolymerizations are effectively identical to those developed for studying the effect of monomer feed rate on the extent of chain transfer to polymer in VAc emulsion homopolymerization.[2] The results from this previous study showed that use of a growth-stage monomer feed rate of 0.35% min^{-1} led to the operation of essentially monomer-starved conditions from the beginning of the growth stage through to completion of the copolymerization. Given that commercial emulsion copolymerizations are usually carried out under monomer-starved conditions to ensure homogeneity of copolymer composition,[14] this feed rate was employed for each of the VAc/BA emulsion copolymerizations reported here. Since the terms *monomer-starved* and *monomer-flooded* conditions often are loosely defined and are important in relation to interpretation of the results from the present studies, they are worthy of further consideration. The most satisfactory means of specifying the monomer-starved condition is to state that the monomer concentration in the particles must be below its equilibrium value for the temperature and pressure of polymerization. However, as in the present work, most researchers do not measure the equilibrium monomer concentration in the particles or the monomer concentration in the particles as a function of conversion, so the most common means of defining monomer-starved conditions is in terms of the instantaneous monomer conversion. This inevitably leads to ambiguities in distinguishing between monomer-starved and monomer-flooded conditions. In the present paper, 80% instantaneous conversion has been used as the nominal demarcation between monomer-starved and monomer-flooded conditions. The demarcation point chosen is not too critical, however, because the crossover from monomer-starved to monomer-flooded conditions will produce a smooth change (not a step change) in the extent of branching. Thus, the terms monomer-starved and monomer-flooded conditions are most useful in highlighting copolymerizations that proceed predominantly under conditions where the mole fraction of monomer in the latex particles is either low or high, respectively.

The variation of instantaneous and overall conversion with reaction time was very similar for each of the copolymerizations, as can be seen from inspection of the representative data shown in Figure 4. The copolymerizations only operated under monomer-flooded conditions during the seed stage, in which 16.7% of the total monomer is polymerized. Hence, the majority (83.3%) of the copolymer was formed under monomer-starved conditions from the beginning of the growth stage onward, the variation of instantaneous conversion with reaction time being similar for each of the emulsion copolymerizations. The results presented and discussed in the following sections will emphasize that, for each copolymerization, the differences in instantaneous conversion during the seed and growth stages lead to significant differences in the detailed structure of the copolymer formed.

VAc/BA Copolymer Triad Sequence Distributions. As described elsewhere,[1,15,16] the spectrum of PVAc homopolymer shows major peaks at 65−68 ppm from CH carbons in regioregular head-to-tail units and minor peaks at 68−71 ppm from CH carbons in head-to-head and tail-to-tail regioirregular units. All peaks show further splittings due to irregular tacticity. In the copolymer spectra, additional CH peaks are observed from different repeat unit sequences; the assignment of these peaks to VAc-centered triads, as indicated in Figure 2, was made on the basis of assignments previously published for VAc/BA copolymers.[9,10,17,18] The VVB triad peaks overlap the peak at 67.7 ppm from regioregular VVV triads and peaks at 68−69 ppm from regioirregular VVV triads, while the BVB triad peak overlaps peaks at 70 ppm from regioirregular VVV triads. To account for this overlap, the VAc-centered triad probabilities were calculated assuming that for each copolymer the ratio of the integral for the regioirregular VVV peaks (which underlie the VVB and VB triad peaks) with respect to the integral for the VVV regioregular peaks at 65−67 ppm is the same as for PVAc homopolymer.

Previous papers[8−10,17,18] have reported the assignment of the complex region of strongly overlapping CH and CH_2 peaks at 32−44 ppm to dyads (CH_2 peaks) and BA-centered triads (CH peaks). The resolution of the sequences is greatly improved by using CH and CH_2 subspectra, as shown for several copolymers in Figures 5 and 6, respectively. These subspectra were obtained by respectively adding and subtracting DEPT spectra obtained with final proton pulse flip angles of 45° and 135°, the relative weighting of the DEPT spectra being

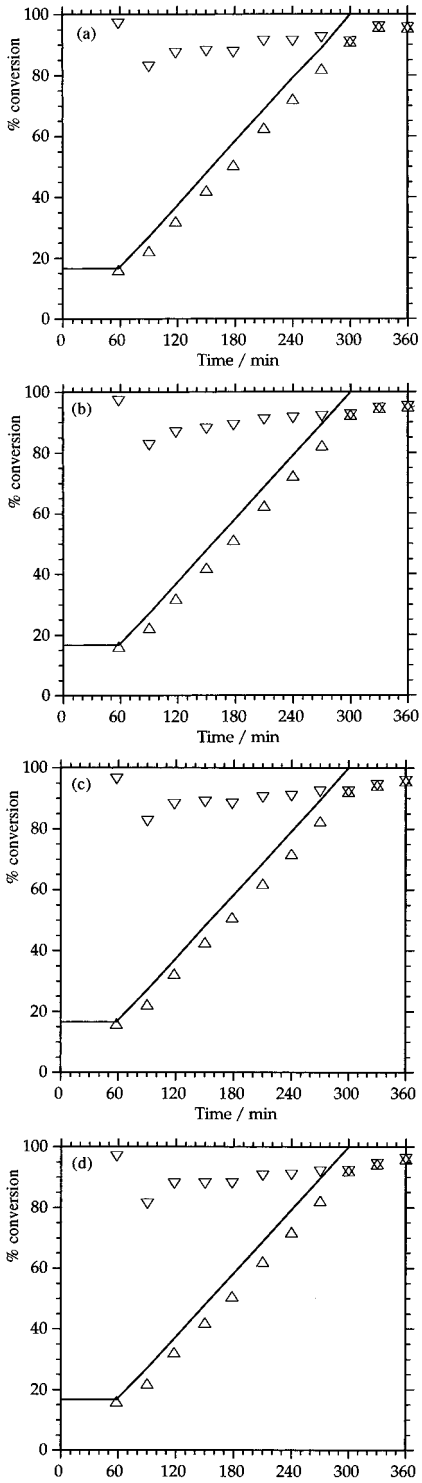

Figure 4. Representative instantaneous conversion (▽) and overall conversion (△) data for the VAc/BA emulsion copolymerizations: (a) 20 wt % BA, (b) 40 wt % BA, (c) 60 wt % BA, and (d) 80 wt % BA.

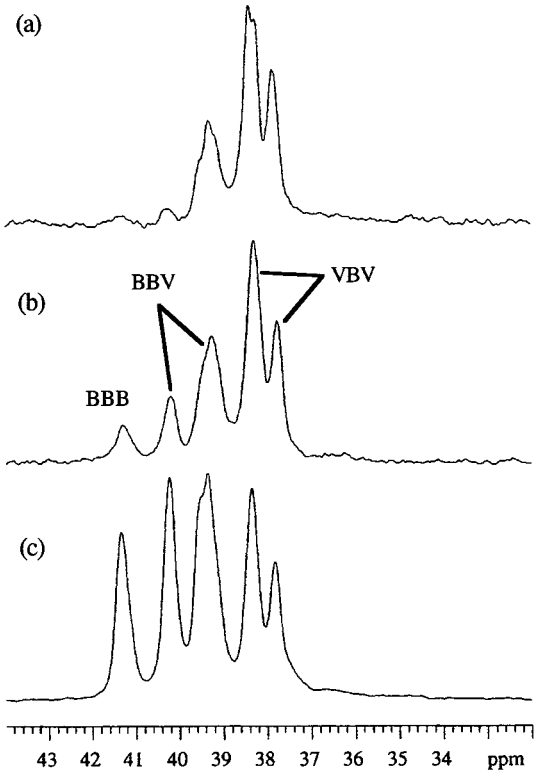

Figure 5. CH subspectra of the 32−44 ppm region of the ^{13}C NMR spectra of final samples from VAc/BA copolymerizations: (a) 15 wt % BA, (b) 40 wt % BA, and (c) 60 wt % BA.

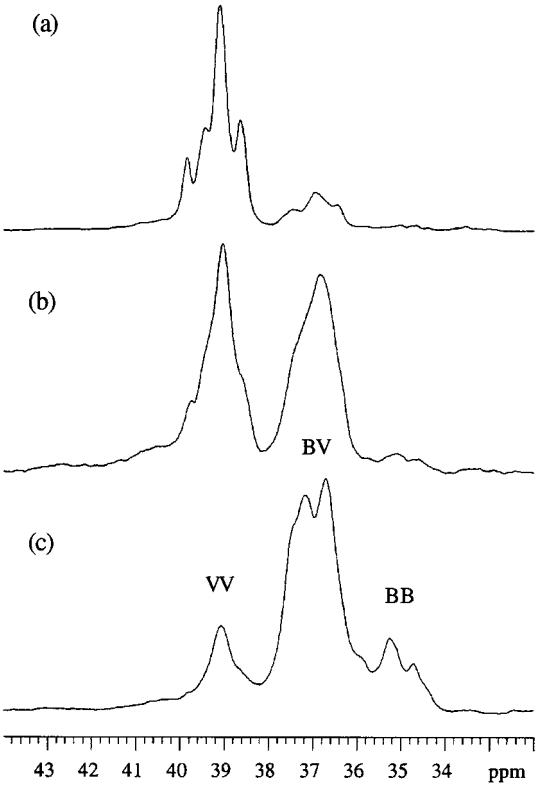

Figure 6. CH_2 subspectra of the 32−44 ppm region of the ^{13}C NMR spectra of final samples from VAc/BA copolymerizations: (a) 15 wt % BA, (b) 40 wt % BA, and (c) 60 wt % BA.

empirically adjusted to null the spectrum intensity at ca. 37 ppm in the CH subspectrum and ca. 41.5 ppm in the CH_2 subspectrum. As indicated in the figures, the CH subspectra show groups of peaks assigned to BA-centered triad sequences, and the CH_2 subspectra show groups of peaks assigned to dyad sequences, the specific assignments having been made on the basis of the variation in peak intensity with composition. Except when the amount of one component is small (<10 mol %), the individual dyad and triad peaks are sufficiently clearly resolved to facilitate reasonably accurate determination of the corresponding sequence probability. Together with the VAc-centered triad probabilities obtained from the CHO peaks as described above, these assignments allow determination of the complete triad

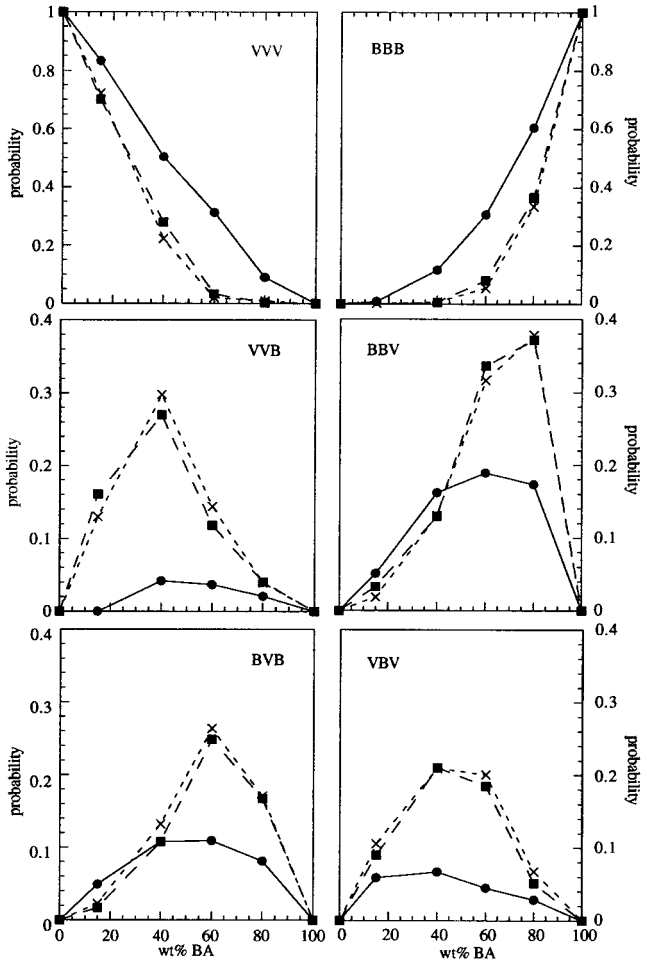

Figure 7. Experimental triad sequence probabilities for VAc/BA copolymers: ●, at the end of the seed stage; ■, the copolymer produced in first half of the growth stage; ×, all of the copolymer produced in growth stage.

distribution of VAc/BA copolymers, which hitherto was severely restricted by overlap of CH and CH_2 carbons in this region.

For each copolymerization, the sequence probabilities calculated from the spectra of the seed-stage copolymer and the final copolymer are considerably different. The differences are even more significant when it is recognized that the sequence distribution for the final copolymers are weighted averages of the distributions for the corresponding growth-stage and seed-stage copolymers, with the latter constituting a significant proportion (16.7%). Clearly, for samples removed during the monomer feed period of the growth stage, the contribution from the seed-stage copolymer is even more marked. To investigate more thoroughly the differences in sequence distribution between the seed-stage and growth-stage copolymers, the sequence probabilities for the copolymer formed *after* the seed stage (referred to here as the *growth-stage copolymer component*) is required and can be determined by eliminating the contribution from the seed-stage copolymer for the samples removed during the growth stage. Thus, the sequence probability, $(X)_{gs}$, of sequence X in the growth-stage copolymer component was calculated using the following equation

$$(X)_{gs} = \frac{(X)_{ov} - x_{ss}(X)_{ss}}{1 - x_{ss}} \tag{5}$$

where $(X)_{ov}$ is the overall probability of sequence X in a copolymer sample removed during the growth stage, $(X)_{ss}$ is the probability of sequence X in the seed-stage copolymer for that copolymerization, and x_{ss} is the mole fraction of the seed-stage component in the growth-stage copolymer sample. The sequence probabilities $(X)_{ov}$ and $(X)_{ss}$ were calculated directly from the ^{13}C NMR spectra of the growth-stage copolymer sample and the corresponding seed-stage copolymer sample, respectively, and x_{ss} was calculated from the overall conversion.

Figure 7 shows the triad sequence distributions determined from the ^{13}C NMR spectra for seed-stage copolymer samples (taken at 60 min reaction time), the growth-stage copolymer component for copolymer samples taken midway through the monomer feed (at 180 min reaction time), and the growth-stage copolymer component for the final copolymers (at 360 min reaction time). For each copolymerization, the distributions for the two growth-stage copolymer components, within experimental error, are effectively identical, indicating that there is no significant change in the copolymerization kinetics during the growth stage. However, in each case, both are very different from that of the corresponding seed-stage copolymer. Although in each case significant proportions of all triads are present (indicating rather irregular microstructures), the growth-stage copolymer components show much higher probabilities of the mixed triads VVB, BVB, BBV, and VBV, whereas the seed-stage copolymers have much higher proportions of the homopolymer triads VVV and BBB. Thus, the growth-stage copolymer components have much more irregular repeat unit sequences than the seed-stage copolymers, which have more blocky microstructures.

Table 2 gives copolymer composition (mol % BA) and dyad probability data calculated from the triad probabilities using eq 6 and eqs 7−9, respectively.

$$(B) = (BBB) + (BBV) + (VBV) \tag{6}$$

$$(VV) = (VVV) + \frac{1}{2}(VVB) \tag{7}$$

$$(BB) = (BBB) + \frac{1}{2}(BBV) \tag{8}$$

$$(BV) = 1 - (VV) - (BB) \tag{9}$$

Taking into account the uncertainties and approximations in the triad separation procedure described at the beginning of this section, there is satisfactory agreement of the calculated mol % BA with that of the monomer feed. The dyad probabilities naturally reflect the trends evident from the triad probabilities and emphasize the distinction between the repeat unit sequencing in the seed-stage copolymer and the growth-stage copolymer components. A randomness factor, *R*, can be calculated from the dyad probabilities as follows:

$$R = \frac{4(VV)(BB)}{(BV)^2} \tag{10}$$

For a Bernoullian sequence distribution, *R* is unity, whereas for tendencies to blockiness or alternation, *R* is greater than or less than unity, respectively. The experimental values of *R* are given in Table 2 and clearly show a significant tendency to blockiness for the seed-stage copolymers and a more random structure

Table 2. Dyad Probabilities and Randomness Factor Calculated from Triad Distributions for the VAc/BA Emulsion Copolymers

monomer feed composition, % BA			exptl copolymer	dyad probability[c]			randomness
wt %	mol %	sample[a]	composition, mol % BA[b]	VV	VB	BB	factor, *R*
15	10.6	seed	12.4	0.787	0.179	0.034	3.3
		mid-feed	11.8	0.781	0.203	0.016	1.2
		final	11.3	0.786	0.203	0.011	0.84
40	30.9	seed	33.7	0.525	0.277	0.198	5.4
		mid-feed	33.1	0.410	0.519	0.071	0.43
		final	35.0	0.372	0.556	0.072	0.35
60	50.2	seed	53.6	0.331	0.267	0.402	7.5
		mid-feed	56.0	0.100	0.680	0.220	0.19
		final	56.0	0.092	0.696	0.212	0.16
80	72.9	seed	77.4	0.111	0.228	0.661	5.6
		mid-feed	76.5	0.022	0.426	0.552	0.27
		final	74.7	0.029	0.447	0.524	0.30

[a] Seed sample: removed at the end of the seed stage (60 min). Mid-feed sample: removed after 180 min, which corresponds to a point approximately midway through the comonomer feed period. Final sample: the copolymer obtained at the end of the reaction. The data for the mid-feed and final samples are for the growth-stage copolymer component (see eq 5 and the related the text). [b] Calculated from the triad probabilities shown in Figure 7 using eq 6. [c] Calculated from the triad probabilities shown in Figure 7 using eqs 7−9.

with a weak tendency toward alternation for the growth-stage copolymer components.

To gain further insight into the copolymerization statistics, the experimental seed-stage copolymer and growth-stage copolymer component triad probabilities are compared in Figures 8 and 9, respectively, with theoretical values calculated as follows.

(i) Triad probabilities calculated for 100% conversion copolymers using the reactivity ratios $r_V = 0.03$ and $r_B = 7$, which are the mean values (taking into account uncertainties) of those determined by Brar and Charan[10] from sequence data for VAc/BA copolymers (prepared by solution copolymerization to <5% conversion in benzene at 60 °C using benzoyl peroxide as initiator). The calculations were made using a simple numerical algorithm in which the copolymerization was simulated by incrementing the conversion up to 100% in steps of 0.01%. The composition and sequence distribution of the copolymer formed in each step was calculated according to the standard terminal-unit first-order Markov statistical model. After each conversion increment, the composition of the residual comonomer mixture was calculated and the procedure repeated. The overall (i.e., cumulative) triad probabilities at 100% conversion are plotted in Figures 8 and 9.

(ii) Triad probabilities calculated using a perfectly random Bernoullian model in which the probabilities of adding each monomer were assumed to be equal to their mole fractions in the feed.

As can be seen from Figure 8, the sequence distribution for copolymer formed in the seed stage is in reasonable agreement with that simulated by model i, suggesting that the reactivities of the growing chain ends and the monomers within the seed particles are not significantly different from those in solution. However, Figure 9 shows that the sequence distribution for copolymer produced in the growth stage is much more closely represented by a random Bernoullian distribution. Such distinctions are in accord with well-established observations on copolymers prepared respectively by batch and monomer-starved semicontinuous batch emulsion copolymerizations.[8,9,14,17−19] In the seed stage, the copolymerizations are operating under monomer-flooded conditions and, on the basis of the established trends, would be expected to follow normal copolymerization kinetics modified only by the effects of monomer partitioning; hence, the reasonable correlation of the

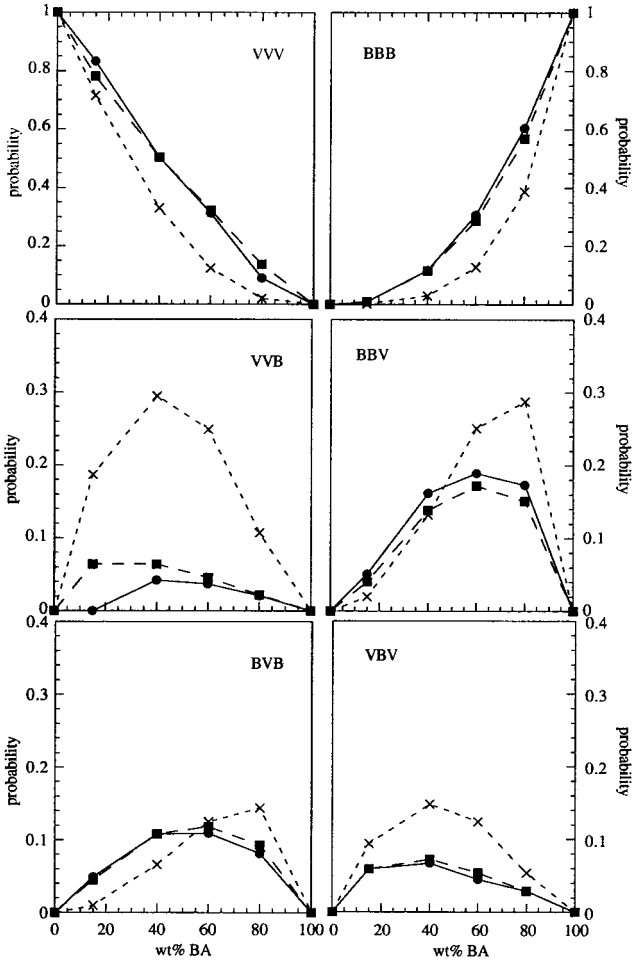

Figure 8. Triad sequence probabilities for VAc/BA copolymers: ●, experimental probabilities for the copolymer at end of the seed stage (this work); ■, simulated probabilities for 100% conversion copolymers with $r_V = 0.03$ and $r_B = 7$ (see text); ×, calculated probabilities for perfectly random copolymers (see text).

seed-stage copolymer sequence distribution with that predicted from reactivity ratios. However, since monomer-starved conditions operate throughout the growth stage, the established trends suggest that the sequence distribution in the growth-stage copolymer components should be random within the constraint that the overall copolymer composition must equal that of the comono-

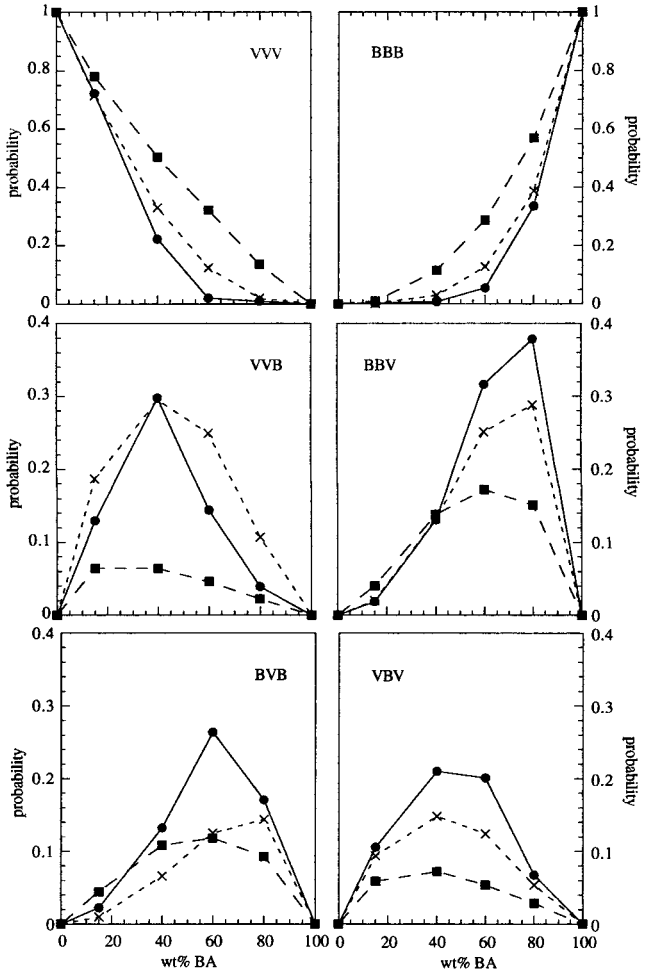

Figure 9. Triad sequence probabilities for VAc/BA copolymers: ●, experimental probabilities for all the copolymer produced in growth stage (this work); ■, simulated probabilities for 100% conversion copolymers with $r_V = 0.03$ and $r_B = 7$ (see text); ×, calculated probabilities for perfectly random copolymers (see text).

mer feed. Again, this prediction is consistent with the observations reported here. While such observations have been reported previously for monomer-starved semicontinuous batch emulsion copolymerizations, the data presented in Figure 9 provide the first unambiguous evidence that copolymer with an essentially random Bernoullian sequence distribution is produced under such conditions.

Although the use of monomer-starved semicontinuous batch emulsion copolymerization for preparation of copolymers with uniform composition is well established,[8,9,14,17−19] the reason why such control is achieved has not been seriously considered. In the present work, the greater resolution of the triad resonances achieved through use of DEPT subspectra and the correction for contributions from the seed-stage copolymer have facilitated more accurate quantification of all six triad sequence probabilities. As indicated above, this has revealed more clearly than in any previous studies that copolymers with random repeat unit sequence distributions are formed under such conditions. Given that normal copolymerization kinetics do not operate and that the random copolymer formed has a composition equal to that of the comonomer feed, the inference to be drawn is that propagation is controlled only by the concentrations of the monomers in the vicinity of the chain radicals, the identity of the end unit of a chain radical being unimportant. This suggests that propagation is subject to diffusion control in emulsion polymerizations operating under monomer-starved conditions. Although such an inference is not consistent with the general thinking on diffusion control of propagation (which usually considers that the system must be glassy for this to occur[20−22]), anomalous behavior has been reported for emulsion polymerization,[23] and there seems no other reasonable explanation of the observed random sequence distribution. As will be explained in the following section, the data on branching lead to exactly the same conclusion.

Effects of Comonomer Composition on Mol % Branches. Before considering the branching data, the factors controlling chain transfer to polymer will be considered briefly. The mole fraction of branched repeat units in polymer formed at a particular instant in time is equal to the probability that a propagating chain radical undergoes chain transfer to polymer rather than propagation, and so for homopolymerizations the mol % branches is given by

$$\text{mol \% branches} = 100 \times \frac{\left(\frac{k_{trP}}{k_p}\right)\frac{[P]}{[M]}}{\left\{\left(\frac{k_{trP}}{k_p}\right)\frac{[P]}{[M]}\right\} + 1} \quad (11)$$

where k_{trP} and k_p are the rate coefficients for chain transfer to a polymer repeat unit and for propagation, respectively, and [P] and [M] are the concentrations of polymer repeat units and monomer, respectively. The two factors that control the extent of chain transfer to polymer and branching in homopolymerizations are, therefore, the rate coefficient ratio k_{trP}/k_p and the concentration ratio [P]/[M]. For copolymerizations, however, there are at least four distinct propagation reactions, and there may also be several possibilities for chain transfer to polymer, so the situation is significantly more complex. Hence, within the constraints of the data available in this work, quantitative correlation of the mol % branches data with the instantaneous conversion data is not feasible. Nevertheless, the same principles are applicable as for homopolymerization; the extent of chain transfer to polymer will be controlled by ratios of rate coefficients for chain transfer to polymer and propagation and by ratios of polymer to monomer concentration, which for emulsion polymerizations need to be considered in terms of the concentrations within the particles (i.e., $[P]_p$ and $[M]_p$) because they are the principal loci for propagation and chain transfer to polymer.

In the present studies, the complexity is reduced because the polymerization temperature was fixed at 70 °C, and the variation of instantaneous conversion with overall conversion is similar for each of the copolymerizations. The fixed temperature makes it reasonable to assume that the rate coefficients for the various propagation and chain transfer to polymer events are constant. However, although the overall ratio $[P]_p/[M]_p$ is controlled principally by the instantaneous conversion, the effects of monomer partitioning between the particles and aqueous phase also need to be considered, especially as partitioning becomes more important when the instantaneous conversion is high.[14] In the present work, the total $[M]_p$ (and hence the overall $[P]_p$/

$[M]_p$) at a given instantaneous conversion can be expected to vary as the comonomer composition changes because VAc has a much greater solubility in water than BA. However, because the instantaneous conversion is calculated in relation to masses of monomer, the much lower molar mass of VAc compared to that of BA will compensate slightly for the effect of its greater partitioning to the aqueous phase when the instantaneous conversion is high. In the following discussion, the effects of comonomer composition on mol % VAc end groups and mol % BA branches are interpreted mainly in terms of the chemistry of chain transfer to polymer and the influence of comonomer composition on the balance between the various competing processes.

For six of the copolymerizations, samples were removed at the end of the seed stage (60 min) and at the midpoint in the monomer feed (180 min). The data from analysis of these copolymers are presented in parts a and b of Figure 10, respectively. The data for the final copolymers from all the emulsion copolymerizations are given in Figure 10c. Comparison of the data in Figure 10a−c for corresponding copolymerizations shows that there is a general trend for $\%V_{ends}/V$ and $\%B_{Cq}/B$ to increase as the overall conversion increases, an observation that is in accord with those from previous studies of emulsion homopolymerizations of VAc and BA.[1,2,4,5] The trend is readily explained in terms of the effects of instantaneous conversion on the overall ratio $[P]_p/[M]_p$, which when averaged over the conversion intervals is much lower for the seed stage than during the growth stage and final period of heating. From eq 11, this must lead to an increase in the frequency of chain transfer to polymer events. More interesting, however, is comparison of the dependence of $\%V_{ends}/V$ and $\%B_{Cq}/B$ on comonomer composition at each of the three times in the copolymerizations. For the final copolymers (Figure 10c) and the samples removed at the midpoint in the monomer feed (Figure 10b), $\%V_{ends}/V$ increases and $\%B_{Cq}/B$ decreases as mol % BA (in the comonomer mixture) increases. However, although the seed stage samples (Figure 10a) show a similar trend for $\%V_{ends}/V$ (which increases with mol % BA), $\%B_{Cq}/B$ is invariant with mol % BA within the scatter of the data. These observations can be interpreted in a self-consistent way in terms of the contribution from chain transfer to polymer involving abstraction of hydrogen atoms from backbone tertiary C−H bonds in BA repeat units by propagating radicals with VAc radical ends, as shown in Scheme 3. Thus, the instantaneous rates of formation of VAc end units and branched BA repeat units are given by the following equations:

$$\frac{d[V_{ends}]}{dt} = \{k_{tr,VB}[PBA] + k_{tr,VV}[PVAc]\}[VAc^\bullet] \quad (12)$$

$$\frac{d[B_{Cq}]}{dt} = \{k_{tr,BB}[BA^\bullet] + k_{tr,VB}[VAc^\bullet]\}[PBA] \quad (13)$$

where $k_{tr,XY}$ are the rate coefficients for chain transfer to polymer involving H-abstraction by a radical with an X end unit from a Y repeat unit (with V and B representing VAc and BA units, respectively), [PVAc] and [PBA] are the concentrations of VAc and BA repeat units, respectively, and [VAc•] and [BA•] are the concentrations of radicals with VAc and BA end units, respectively.

The data presented in Figure 10b,c will be considered in relation to eqs 12 and 13 first because they correspond to the growth stage of the copolymerizations which operated under monomer-starved conditions, for which the equations can be further simplified to the following forms (see the Appendix)

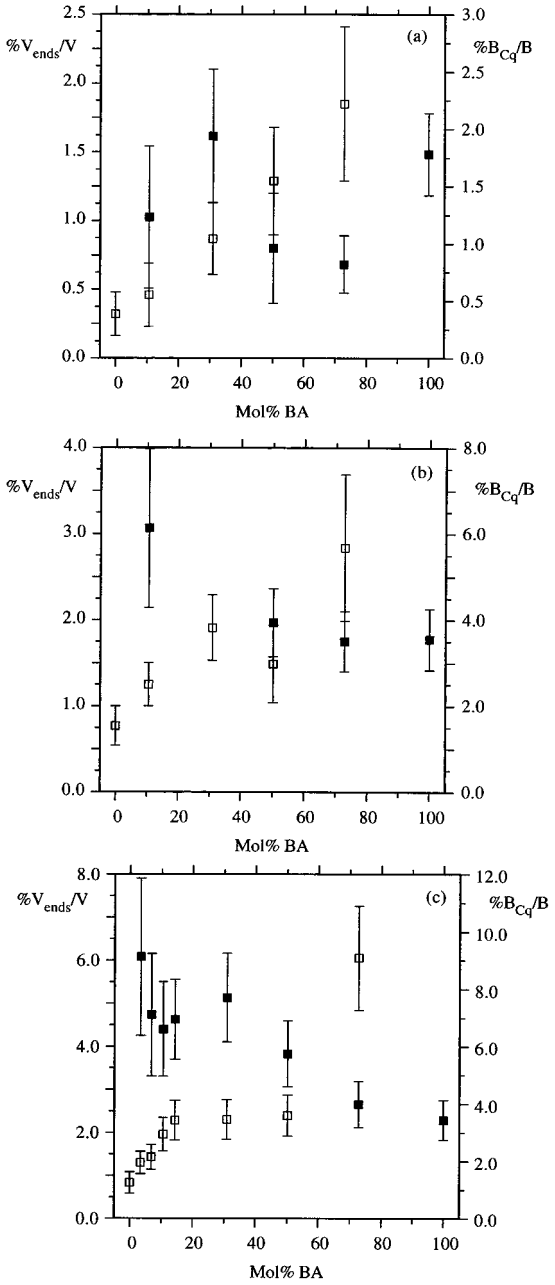

Figure 10. Variation of $\%V_{ends}/V$ (□) and $\%B_{Cq}/B$ (■) with mol % BA for (a) the copolymers at the end of the seed stage, (b) the copolymers at the midpoint in the growth stage, and (c) the final copolymers. (The $\%B_{Cq}/B$ data for the copolymer at the midpoint in the growth stage for the copolymerization at 40 wt % BA (30.9 mol % BA) were unreliable and so are not included.)

$$\frac{d(\%V_{ends}/V)}{dt} = 100K\{(k_{tr,VB} - k_{tr,VV})[BA]_{mol\%} + 100k_{tr,VV}\}, \quad \text{for } [BA]_{mol\%} < 100 \quad (14)$$

$$\frac{d(\%B_{Cq}/B)}{dt} = 100K\{(k_{tr,BB} - k_{tr,VB})[BA]_{mol\%} + 100k_{tr,VB}\}, \quad \text{for } [BA]_{mol\,\%} > 0 \quad (15)$$

in which $[BA]_{mol\%}$ is the mol % of BA in the comonomer

Scheme 3. Mechanism of Chain Transfer to Polymer Involving Abstraction of Hydrogen Atoms from Backbone Tertiary C−H Bonds in BA Repeat Units by Propagating Radicals with VAc Radical Ends (Carbons Labeled A and B Are Described in the Discussion and Are Identical with Those Labeled Similarly in Schemes 1 and 2)

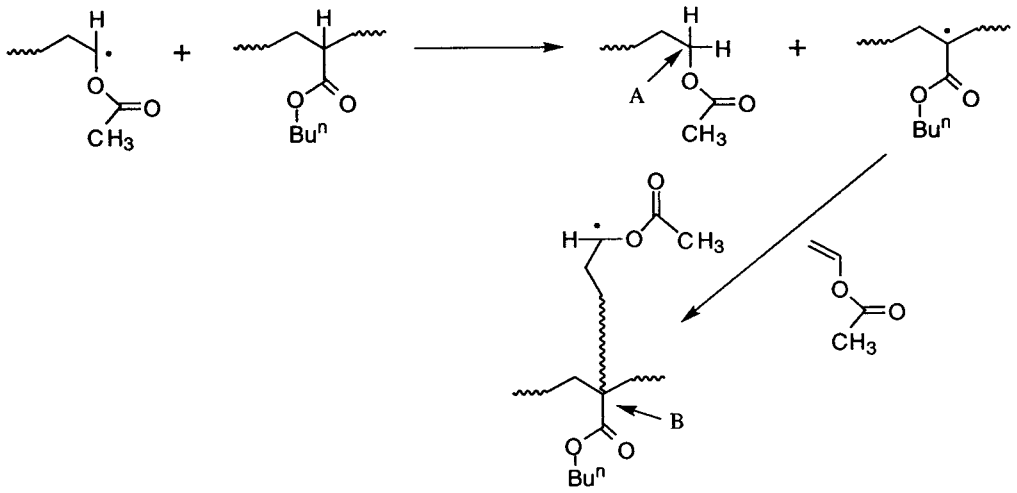

mixture within the particles and K is a constant for a particular emulsion copolymerization. The equations are linear in $[BA]_{mol\%}$ and effectively give the instantaneous values of $\%V_{ends}/V$ and $\%B_{Cq}/B$ as functions of $[BA]_{mol\%}$ within the limits indicated. Semiquantitative interpretation of the trends observed for the variation of $\%V_{ends}/V$ and $\%B_{Cq}/B$ with [BA] is made possible by assuming that the quantities on the right-hand sides of the equations have constant values, in which case the differential quantities on the left-hand side are proportional to the measured values of $\%V_{ends}/V$ and $\%B_{Cq}/B$. Though not rigorous, this assumption is not too unreasonable for copolymerization under monomer-starved conditions. On this basis, the data in Figure 10b,c are consistent with the equations in that, within the experimental error, there are nominally linear variations in $\%V_{ends}/V$ and $\%B_{Cq}/B$ as $[BA]_{mol\%}$ increases. The observations that $\%V_{ends}/V$ increases and $\%B_{Cq}/B$ decreases as $[BA]_{mol\%}$ increases indicate that k_{trVB} is greater than both k_{trVV} and k_{trBB}, showing that there is synergism in chain transfer to polymer for copolymerization of VAc and BA. By fitting linear regression lines through the experimental data and correlating the lines to eqs 14 and 15 with the differential quantities replaced by $\%V_{ends}/V$ and $\%B_{Cq}/B$, respectively, values of k_{trVB}, k_{trVV}, and k_{trBB} can be obtained, but only in terms of the proportionality constants and so are not meaningful. However, this procedure does allow calculation of the ratios of their values which are worthy of more detailed consideration: (i) from Figure 10b $k_{trVB} > k_{trBB} > k_{trVV}$ with $k_{trVB}/k_{trVV} \approx 7$ and $k_{trVB}/k_{trBB} \approx 4$; (ii) from Figure 10c $k_{trVB} > k_{trBB} > k_{trVV}$ with $k_{trVB}/k_{trVV} \approx 8$ and $k_{trVB}/k_{trBB} \approx 3$. This approximate analysis, therefore, indicates that radicals with VAc end units abstract hydrogen atoms from BA repeat units about 7−8 times more rapidly than from VAc repeat units and that radicals with VAc end units are about 3−4 times as effective in abstracting hydrogen atoms from BA repeat units than are radicals with BA end units. Thus, even at low levels of BA, the chemistry shown in Scheme 3 has very significant effects on the level of branching, which increases substantially with BA content due mainly to branching at BA repeat units arising from H-abstraction by propagating radicals with VAc ends.

The distinctive feature of the data for the copolymers from the seed stages of the copolymerizations is that

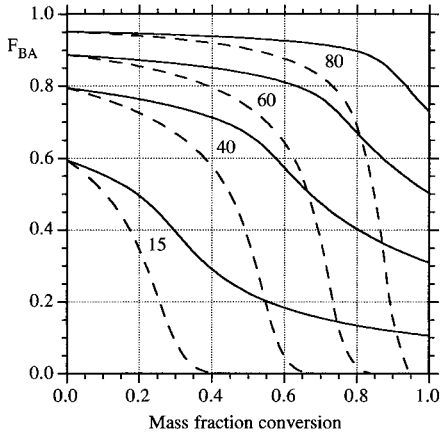

Figure 11. Simulations of the variation of instantaneous (broken lines) and cumulative (solid lines) copolymer composition, F_{BA} (mole fraction of BA units), with the total mass fraction conversion for VAc/BA copolymerizations with initial comonomer compositions of 15, 40, 60, and 80 wt % BA, as indicated (see text).

although $\%V_{ends}/V$ increases with mol % BA (as observed for the growth-stage copolymers), $\%B_{Cq}/B$ does not vary with mol % BA. To interpret these data without introducing new concepts, the "batch" nature of the seed stage must be taken into account. All monomer required for the seed stage is added at the beginning and then allowed to achieve essentially complete conversion during the seed stage. Thus, in the seed stage, the copolymerization proceeds under monomer-flooded conditions, and copolymer composition drift can be expected, as is evident from the sequence distribution data. The variation of copolymer composition with conversion under such conditions was simulated using the same reactivity ratios and numerical algorithm described above for simulation of the monomer sequence distribution. This procedure was carried out for each of the initial BA compositions at which seed-stage branching data were obtained. The resulting simulations of instantaneous and cumulative copolymer composition are shown in Figure 11 plotted against the mass fraction conversion (rather than mole fraction conversion) since this relates directly to the measured conversions and allows for easier interpretation. Chain transfer to polymer will be most significant when the concentration of copolymer in the particles attains high values, i.e., at high mass

fraction conversions. As can be seen from the curves in Figure 11, when the mass fraction conversion is high (e.g., above 0.8), virtually all of the BA has reacted. Hence, in the latter period of the reaction when most of the branching due to chain transfer to polymer takes place, radicals with VAc ends predominate almost to the complete exclusion of radicals with BA ends. Thus, a reasonable assumption is that radicals with VAc ends are responsible for most of the branching present in the seed-stage copolymers and that the branching occurs in the period during which the mass fraction conversion increases from 0.8. The incidence of chain transfer to polymer via the chemistry shown in Scheme 3 will increase with the concentration of BA repeat units and, given the approximately 7−8 times higher rate at which radicals with VAc end units abstract hydrogen from BA repeat units than from VAc repeat units, the value of $\%V_{ends}/V$ should increase approximately linearly with BA concentration, as observed. However, the radicals with VAc end units sample the same *proportion* of the available BA repeat units in each case and so the value of $\%B_{Cq}/B$ does not vary with the concentration of BA repeat units, again as observed.

Thus, the principal distinction between branching in the seed stage and the growth stage is that, for the former, chain transfer to polymer arises almost exclusively from radicals with VAc end units (as a consequence of the monomer-flooded conditions), whereas for the latter, radicals with BA end units and radicals with VAc end units both contribute to chain transfer to polymer in proportions that correspond to the composition of the comonomer feed (as a consequence of the monomer-starved conditions).

Conclusions

Although the initial aim of the work described in this paper was simply to determine the effect of comonomer composition on branching in VAc/BA emulsion copolymerizations, much more has been achieved and the results have led to several conclusions that were not anticipated when the work was originated.

The emulsion copolymerizations proceeded via a seed stage that was carried out under monomer-flooded conditions, followed by a growth stage that operated under monomer-starved conditions. The ^{13}C NMR spectra of the copolymers have been fully interpreted in terms of both the structural features arising from chain transfer to polymer and the repeat unit sequence distributions. The results for the seed-stage and growth-stage copolymers are distinctly different and provide new insight into the kinetics of the copolymerization and chain transfer to polymer.

The sequence distributions for the copolymers formed in the seed stages are in reasonable agreement with those predicted from published reactivity ratios using the standard terminal-unit first-order Markov statistical model. This is expected because, under monomer-flooded conditions, the normal copolymerization kinetics should be modified only by the effects of monomer partitioning. However, in each case, the sequence distribution for the copolymer produced in the growth stage is much more closely represented by a random Bernoullian distribution, this being a consequence of the monomer-starved conditions. Although such observations have been reported previously, the results presented here show, more clearly than any previous studies, that copolymers with random repeat unit sequence distributions are formed under monomer-starved conditions. Despite its significance, the underlying reasons for this observation have not been considered in previous studies. Such considerations are, however, important, and the fact that random copolymer with a composition equal to that of the comonomer feed is formed under monomer-starved conditions leads to the inference that propagation is controlled only by the concentrations of the monomers in the vicinity of the chain radicals, the identity of the end unit of a chain radical being unimportant. The only reasonable explanation of this observation is that propagation is subject to diffusion control in emulsion copolymerizations operating under monomer-starved conditions, even though this interpretation is in contradiction with present thinking on diffusion control of propagation for homogeneous polymerizations.

The branching data for the copolymers reveal that a synergistic effect exists in which the inclusion of only small amounts of either monomer leads to disproportionate increases in the level of branching. These increases are a consequence of the efficacy of H-abstraction at BA backbone tertiary C−H bonds by the highly reactive VAc-ended chain radicals. The results indicate that radicals with VAc end units abstract hydrogen atoms from BA repeat units about 7−8 times more rapidly than from VAc repeat units and that radicals with VAc end units are about 3−4 times as effective in abstracting hydrogen atoms from BA repeat units than are radicals with BA end units. Thus, by copolymerizing VAc with relatively small amounts of BA (which is common practice in commercial VAc-based emulsion polymerizations), the relatively high susceptibility of acrylic tertiary C−H bonds to abstraction leads to significant increases in the total level of branching in the copolymers produced. Additionally, from the perspective of acrylic polymers, the presence of VAc leads to a much higher level of acrylic branch points than would occur in an all-acrylate polymerization. As for the sequence distribution data, there are significant differences in the data for the seed-stage and growth-stage copolymers. Copolymer composition drift occurs in the seed stage due to the monomer-flooded conditions and results in virtually all of the BA being consumed before the conversion is high enough for chain transfer to polymer to become significant; hence, branching arises almost exclusively from H-abstractions by radicals with VAc end units. However, in the monomer-starved growth stage, radicals with BA end units and radicals with VAc end units both contribute to chain transfer to polymer in proportions that correspond to the composition of the comonomer feed. The latter observation again is consistent with diffusion control of propagation under monomer-starved conditions.

Acknowledgment. The authors thank the Engineering and Physical Sciences Research Council for funding the work described in this paper through award of Grants GR/L02494 and GR/L02623.

Appendix

Equations 12 and 13 can be simplified for copolymerizations that operate under monomer-starved conditions by making a series of assumptions that lead to further equations which allow greater insight into the contributions to chain transfer to polymer and facilitate semiquantitative interpretation of the trends observed for the variation of $\%V_{ends}/V$ and $\%B_{Cq}/B$ with [BA]. The

development of eqs 12 and 13 into forms that are useful for this purpose is given here in some detail in order to assist the reader in following the logic applied and also to highlight the assumptions and their limitations. It should be stressed, however, that the assumptions lead to nonrigorous equations which should not be applied without due caution for interpretation of other data.

For comparison with the experimentally determined branching levels, it is convenient to convert the concentrations $[V_{ends}]$, $[B_{Cq}]$, [PBA], and [PVAc] into mol % quantities by dividing both sides of each of eqs 12 and 13 by {([PBA] + [PVAc])/100} to give

$$\frac{d[V_{ends}]_{mol\%}}{dt} = \{k_{tr,VB}[PBA]_{mol\%} + k_{tr,VV}[PVAc]_{mol\%}\}[VAc^\bullet] \quad (A1)$$

$$\frac{d[B_{Cq}]_{mol\%}}{dt} = \{k_{tr,BB}[BA^\bullet] + k_{tr,VB}[VAc^\bullet]\}\{PBA\}_{mol\%} \quad (A2)$$

where the additional subscripts indicate the quantities that are now given in mol %. This conversion is reasonable for the monomer-starved conditions of the growth stage because the quantity ([PBA] + [PVAc]) is approximately constant. Since these equations contain terms in radical concentrations, however, they need to be developed further for use in data interpretation.

As shown by the sequence distribution data, under the monomer-starved conditions of the growth stages, the molar ratios of the two types of radicals (with VAc and BA end units) will be equal to the molar ratios of the respective monomers in the latex particles which in turn will reflect the composition of the comonomer mixture and the copolymer, i.e.

$$[PVAc]_{mol\%} = [VAc]_{mol\%} \quad \text{and} \quad [PBA]_{mol\%} = [BA]_{mol\%} \quad (A3)$$

and

$$\frac{[BA^\bullet]}{[VAc^\bullet]} = \frac{[PBA]}{[PVAc]} = \frac{[PBA]_{mol\%}}{[PVAc]_{mol\%}} = \frac{[BA]}{[VAc]} = \frac{[BA]_{mol\%}}{[VAc]_{mol\%}} \quad (A4)$$

from which, in accordance with Bernoullian statistics, the following relationships can be deduced:

$$[VAc^\bullet] = K[PVAc]_{mol\%} \quad \text{and} \quad [BA^\bullet] = K[PBA]_{mol\%} \quad (A5)$$

where K is a constant for a particular emulsion copolymerization. Substituting for the radical concentration terms in eqs A1 and A2 using the relations given in eq A5 gives

$$\frac{d[V_{ends}]_{mol\%}}{dt} = K\{k_{tr,VB}[PBA]_{mol\%} + k_{tr,VV}[PVAc]_{mol\%}\}[PVAc]_{mol\%} \quad (A6)$$

$$\frac{d[B_{Cq}]_{mol\%}}{dt} = K\{k_{tr,BB}[PBA]_{mol\%} + k_{tr,VB}[PVAc]_{mol\%}\}[PBA]_{mol\%} \quad (A7)$$

Equations for the quantities $\%V_{ends}/V$ and $\%B_{Cq}/B$ can be generated by dividing $[V_{ends}]_{mol\%}$ and $[B_{Cq}]_{mol\%}$ by ($[PVAc]_{mol\%}$/100) and ($[PBA]_{mol\%}$/100), respectively. In this way, and through further rearrangements made possible using the relationships given in eq A3 and the relationship $[PBA]_{mol\ \%} + [PVAc]_{mol\ \%} = 100$, eqs A6 and A7 can be converted to the normalized forms for monomer-starved conditions given earlier as eqs 14 and 15.

References and Notes

(1) Britton, D.; Heatley, F.; Lovell, P. A. *Macromolecules* **1998**, *31*, 2828.
(2) Britton, D.; Heatley, F.; Lovell, P. A. *Macromolecules* **2000**, *33*, 5048.
(3) Lovell, P. A.; Shah, T. H.; Heatley, F. *Polym. Commun.* **1991**, *32*, 98.
(4) Lovell, P. A.; Shah, T. H.; Heatley, F. *Polym. Mater. Sci. Eng.* **1991**, *64*, 278.
(5) Lovell, P. A.; Shah, T. H.; Heatley, F. In *Polymer Latexes: Preparation, Characterisation and Applications*; Daniels, E. S., Sudol, E. D., El-Aasser, M. S., Eds.; ACS Symp. Ser. Vol. 492; American Chemical Society: Washington, DC, 1992; Chapter 12, p 188.
(6) Ahmad, N. M.; Heatley, F.; Lovell, P. A. *Macromolecules* **1998**, *31*, 2822.
(7) Vandezande, G. A.; Smith, O. W.; Bassett, D. R. In *Emulsion Polymerization and Emulsion Polymers*; Lovell, P. A., El-Aasser, M. S., Eds.; John Wiley & Sons: Chichester, 1997; Chapter 16, p 563.
(8) Kong, X.-Z.; Pichot, C.; Guillot, J.; Cavaille, J. Y. In *Polymer Latexes: Preparation, Characterisation and Applications*; Daniels, E. S., Sudol, E. D., El-Aasser, M. S., Eds.; ACS Symp. Ser. Vol. 492; American Chemical Society: Washington, DC, 1992; Chapter 11, p 163.
(9) Kong, X.-Z.; Yuan, Q.; Kan, C.-Y. *Acta Polym. Sinica* **1995**, *6*, 308.
(10) Brar, A. S.; Charan, S. *J. Polym. Sci., Polym. Chem.* **1995**, *33*, 109.
(11) Doddrell, D. M.; Pegg, D. T.; Bendall, M. R. *J. Magn. Reson.* **1982**, *48*, 323.
(12) Breitmaier, E.; Voelter, W. *Carbon-13 NMR Spectroscopy*, 3rd ed.; VCH Publishers: Weinheim, Germany, 1987; p 50.
(13) Breitmaier, E.; Voelter, W. *Carbon-13 NMR Spectroscopy, 3rd ed.;* VCH Publishers: Weinheim, Germany, 1987; p 315.
(14) Lovell, P. A. In *Emulsion Polymerization and Emulsion Polymers*; Lovell, P. A., El-Aasser, M. S., Eds.; John Wiley & Sons: Chichester, United Kingdom, 1997; Chapter 7, p 239.
(15) Ketels, H.; Beulen, J.; van der Velden, G. *Macromolecules* **1988**, *21*, 2032.
(16) Amiya, S. In *Progress in Pacific Polymer Science 3*; Ghiggino, K. P., Ed.; Springer-Verlag: Berlin, 1994; p 367.
(17) El-Aasser, M. S.; Makgawinata, T.; Misra, S.; Vanderhoff, J. W.; Pichot, C.; Llauro, M. F. In *Emulsion Polymerization of Vinyl Acetate*; El-Aasser, M. S., Vanderhoff, J. W.; Eds.; Applied Science Publishers: London, 1981; Chapter 12, p 215.
(18) Pichot, C.; Llauro, M. F.; Pham, Q.-T. *J. Polym. Sci., Polym. Chem.* **1981**, *19*, 2619.
(19) Guillot, J. *Makromol. Chem., Suppl.* **1985**, *10/11*, 235.
(20) Casey, B. S.; Mills, M. F.; Sangster, D. F.; Gilbert, R. G.; Napper, D. H. *Macromolecules* **1992**, *25*, 7063.
(21) Maxwell, I. A.; Russell, G. T. *Makromol. Chem., Theory Simul.* **1993**, *2*, 95.
(22) Litvinenko, G. I.; Kaminsky, V. A. *Prog. React. Kinet.* **1994**, *19*, 139.
(23) Faldi, A.; Tirrell, M.; Lodge, T. P.; von Meerwall, E. *Macromolecules* **1994**, *27*, 4184.

MA000901S